

# Different N-terminal isoforms of Oct-1 control expression of distinct sets of genes and their high levels in Namalwa Burkitt's lymphoma cells affect a wide range of cellular processes

Elizaveta V. Pankratova<sup>\*†</sup>, Alexander G. Stepchenko<sup>†</sup>, Tatiana Portseva, Vladic A. Mogila and Sofia G. Georgieva<sup>\*</sup>

Department of Transcription Factors, Engelhardt Institute of Molecular Biology, Russian Academy of Sciences, Vavilov Str. 32, Moscow 119991 Russia

Received October 14, 2015; Revised June 28, 2016; Accepted July 01, 2016

## ABSTRACT

**Oct-1 transcription factor has various functions in gene regulation. Its expression level is increased in several types of cancer and is associated with poor survival prognosis. Here we identified distinct Oct-1 protein isoforms in human cells and compared gene expression patterns and functions for Oct-1A, Oct-1L, and Oct-1X isoforms that differ by their N-terminal sequences. The longest isoform, Oct-1A, is abundantly expressed and is the main Oct-1 isoform in most of human tissues. The Oct-1L and the weakly expressed Oct-1X regulate the majority of Oct-1A targets as well as additional sets of genes. Oct-1X controls genes involved in DNA replication, DNA repair, RNA processing, and cellular response to stress. The high level of Oct-1 isoforms upregulates genes related to cell cycle progression and activates proliferation both in Namalwa Burkitt's lymphoma cells and primary human fibroblasts. It downregulates expression of genes related to antigen processing and presentation, cytokine-cytokine receptor interaction, oxidative metabolism, and cell adhesion, thus facilitating pro-oncogenic processes.**

## INTRODUCTION

Oct-1 (gene symbol *POU2F1*) is a member of the POU domain DNA-binding transcription regulators of higher eukaryotes (1–4). The Oct-1 POU domain interacts as a monomer with an octamer motif ATGCAAAT (2) and related sequences (5–9). It also acts as a dimer, binding to a variety of palindromic sequences such as PORE or MORE (10). Oct-1 controls a wide range of targets including house-

keeping genes (11–14), as well as genes specific for the immune, endocrine, and nervous systems (2,15–19). Oct-1 is also involved in stress response. The Oct-1 hypomorphic embryonic fibroblasts are hypersensitive to oxidative and genotoxic stresses (20). It was demonstrated that under stress conditions the conserved amino acid residues in the Oct-1 DNA-binding domain are phosphorylated altering its affinity to the binding sites (21). Finally, high Oct-1 levels are found in somatic and cancer stem cells (22). Oct-1 is considered to be one of the major regulators of normal and cancer stem cell function (22,23). Oct-1 shares a significant homology with Oct-4, the master regulator of stem cells, including the same gene targets and binding sites, and associated processes (23).

Recent studies demonstrate an important role of high levels of Oct-1 and its prognostic value in the malignant tumor development. Oct-1 controls stem cell markers in multiple tumor cell lines. It promotes tumor engraftment and hematopoietic stem cell engraftment potential in transplants (22). An increased Oct-1 expression level is found in breast adenocarcinoma (22), cervix cancer (24), and in gastric cancer (25). A statistically significant increase in the Oct-1 mRNA level is found in several cancer types (ONCOMINE database). Oct-1 overexpression is strongly associated with a poor survival of patients with gastric cancer, and the 5-year survival rate in the Oct-1 high group (8.9%) was substantially lower than that of the Oct-1 low group (51.1%). A stratification by the Oct-1 expression level displayed an even higher prognostic significance than the widely employed AJCC staging (25). However, at present time there is a lack of data that may explain tumorigenic effect of Oct-1 at the molecular level. In mice, the low level of Oct-1 may cause metabolic changes that are opposed to the anaerobic glycolytic metabolism frequently implicated in the malignant transformation (26).

<sup>\*</sup>To whom correspondence should be addressed. Tel: +7 499 135 9729; Fax: +7 499 135 1405; Email: pank@eimb.ru  
Correspondence may also be addressed to S.G. Georgieva. Email: sonjag@molbiol.edu.ru

<sup>†</sup>These authors contributed equally to the work as first authors.

A variety of genes and processes controlled by Oct-1 suggests that they may be controlled by specific and distinct Oct-1 isoforms. Indeed, 15 alternative human Oct-1 (*POU2F1*) transcripts are annotated in The Genome Annotation for Alternative Splicing Database (<http://genome.ewha.ac.kr/ECgene>). Previously, we studied Oct-1A, Oct-1L, and Oct-1X and have demonstrated that they start from alternative promoters of the *POU2F1* gene and the predicted isoforms differ by their N-termini (27–29). At present time, the ‘canonical’ Oct-1 protein is considered to be a sequence of 743 aa corresponding to Oct-1X (UniProt, P14859-1). The Oct-1A transcript (NM\_002697) contains an open reading frame for Oct-1A protein (766 aa, UniProt P14859-6) which represents the longest form of Oct-1 comprising all the internal exons (30). The Oct-1L (AY113189) (755 aa, UniProt P14859-2) transcript is tissue-specific (31) while Oct-1X mRNA, which we described earlier (KT438684.1) is expressed at a low level in most tissues (29). Still, the presence of specific Oct-1 protein isoforms in mammalian tissues was not investigated and their functions are unknown.

Here, we identified the Oct-1A, Oct-1L, and Oct-1X protein isoforms in human cells, compared gene expression profiles controlled by different isoforms, and investigated connection of high level of Oct-1 expression with different processes in the Burkitt’s lymphoma and normal human cells. We raised antibodies which specifically recognize Oct-1A and Oct-1L isoforms and demonstrated their existence in human tissues for the first time. We showed that the abundantly expressed Oct-1A is the main Oct-1 isoform in the majority of human tissues while the ‘canonical’ Oct-1X isoform is expressed at a very low level relative to Oct-1A. A high level of Oct-1L was found in B-cell tumor lines.

Overexpression of Oct-1 isoforms in the Namalwa Burkitt’s lymphoma cell line and the subsequent functional enrichment analysis of differentially expressed genes (DEGs) demonstrated similarity as well as significant differences in the gene expression patterns and processes controlled by distinct isoforms. Oct-1X, in contrast to other isoforms, regulates genes involved in DNA replication, DNA repair, RNA processing and cellular response to stress. High level of Oct-1 isoforms in cells upregulates genes related to cell cycle progression and activates proliferation both in Namalwa cells and primary human fibroblasts. It also downregulates cell adhesion, cytokine-cytokine receptor interaction, antigen processing and presentation, and impairs the mitochondrial function. Thus, our study reveals pathways and processes stimulated by Oct-1 in Burkitt’s lymphoma and normal human fibroblasts. The high level of Oct-1 also represses genes involved both in positive and negative regulation of apoptosis and its influence on apoptosis depends on the cell type and cell growth conditions. In addition, we have demonstrated that overexpression of Oct-1 isoforms promotes the pro-apoptotic effect of camptothecin in the Namalwa Burkitt’s lymphoma cells.

## MATERIALS AND METHODS

### Cell culture and transduction of human cells

The human cell line, Burkitt’s lymphoma Namalwa (Russian Cell Culture Collection, Institute of Cytology, St. Pe-

tersburg, Russia) and primary human fibroblasts (HFs), obtained from a healthy donor with an informed consent, according to the Institutional Ethics Committee Guidelines. Cells were maintained in DMEM with 10% FCS, 100 U/ml penicillin, 100 µg/ml streptomycin. ViraPower Lentiviral Expression System (Invitrogen) was used for a stable transduction of cells according the manufacturer’s protocol. Blasticidin was used to maintain the stably transformed cells and withdrawn from the media 3 days before the experiment.

### Constructs

The constructs, pL-Oct-1A-3FLAG, pL-Oct-1L-3FLAG, pL-Oct-1X-3FLAG (C-end) were generated by inserting a copy of human Oct-1 coding sequences into the pLenti6/V5-D-TOPO expression vector (Invitrogen).

### RNA purification and qRT-PCR analysis

RNA from cell lines was purified with Trizol. Human tissue-specific RNA was from FirstChoice Human Total RNA Survey Panel (Ambion). Reverse transcription was performed with Maxima First Strand cDNA Synthesis Kit for RT-qPCR (Thermo Scientific) and PCR with the qPCRmix-HS-SYBR (Evrogen). Primers used: Oct-1A Forw5’-TATTCAAATGGCGGACGGA-3’; Oct-1 Forw5’-CCACCCCAAAGTCTACCTGT-3’; Oct-1X Forw5’-CAGCACGATTTGTTGGATGTG-3’; Rev5’-GTTTCTGACGGATTGTTTCATTC-3’. The mRNA levels were normalized to that of 18S RNA gene. Measurements at each point were made in at least three replicates, and the mean value was calculated.

### Gene expression analysis

Microarrays were processed by Genoanalytica (Moscow, Russian Federation) on Illumina HumanHT-12V4 Chips (47 300 sequences) and processed using Illumina GenomeStudio Data Analysis Software and Gene Expression module (version 1.1.1). The *P*-values for differential expression were calculated using the Illumina Custom Error Model algorithm and the Benjamini and Hochberg false discovery rate (FDR), a multiple testing correction method for adjustment of the *P*-values. Changes in gene transcription were deemed as significant based on a fold change of  $\geq 2.0$  and a Benjamini–Hochberg adjusted  $P \leq 0.01$ . For microarray experiments, Namalwa and the empty lentivirus transformed cells were used as controls, and no statistically reliable differences between them were found.

### In vitro transcription and translation of Oct-1 isoforms

The plasmids, Oct-1A/pcDNA3.1, Oct-1L/pcDNA3.1, and Oct-1X/pcDNA3.1 were transcribed and translated according to the manual of TNTR coupled Reticulocyte Lysate system (Promega). The synthesized proteins were resolved by 8% SDS–PAGE and visualized by western blot analysis using mouse anti-FLAG antibody.

## Functional enrichment analysis of DEGs

Gene Ontology screening was performed (GO; DAVID (david.abcc.ncifcrf.gov/home.jsp): GOTERM\_BP\_FAT (biological process), GOTERM\_MF\_FAT (molecular function), GOTERM\_CC\_FAT (cellular component), and KEGG Pathway ([www.genome.jp/kegg/pathway.html](http://www.genome.jp/kegg/pathway.html))). DAVID calculates a modified Fisher's Exact *P*-value to demonstrate GO or molecular pathway enrichment. The *P*-value of <0.05 was chosen as the cut-off criterion.

## Antibodies

Rabbits were immunized with synthetic peptides linked to PEGylated KHL. The antibodies were precipitated with ammonium sulfate and depleted from anti-KHL antibodies on an affinity column. To avoid cross-reaction, anti-Oct-1A antibody was passed through an affinity column with bound Oct-1L specific peptide and vice versa. Each antibody specifically recognized the corresponding peptide on western blots.

## Measuring proliferation capacity of cells

Live cells were stained with CellTrace™ Violet Cell Proliferation Kit (Invitrogen) according to the manufacturer's protocol before plating into the wells. The fluorescence of live cells was measured at 0, 24, and 48 h after plating, on a Beckman Coulter Epix XL4 flow cytometer. CellTiter assay (Promega) which is more appropriate for a long time cell monitoring was used for determination of the relative cell division rate of HF. HF were plated at 5000 cells/well into each well of a 96-well plate, and CellTiter readings were taken every day for 10 days.

## Determination of apoptosis by flow cytometry

Apoptosis was verified by double staining with the AnnexinV-FITC (Molecular Probes) and propidium iodide. The distribution of cells according to their fluorescence was determined for viable and apoptotic subpopulations, which were separated by size and granularity. All measurements were carried out on a Beckman Coulter Epix XL4 flow cytometer.

## Bioluminescence caspase 3/7 assay

Namalwa cells were plated in 96-well plates and treated with camptothecin (2  $\mu$ M) for 18 h or left untreated. Caspase-Glo-3/7 Reagent was added to the wells and incubated at room temperature for 60 min. The luminescence of each sample was measured in a plate-reading luminometer as directed by the luminometer manufacturer. Results were plotted as signal-to-noise ratios. Background readings were determined from wells containing culture medium without cells.

## Statistics

Statistical analysis was performed using Microsoft Excel and Graph Pad Prism. The unpaired Student's *t*-test was used to generate *P* values. Error bars represent S.E.M. (\**P* < 0.05, and \*\**P* < 0.01).

## RESULTS

### Oct-1 isoforms with different N-terminal sequences are present in human cells

Here we studied the three Oct-1 isoforms (Oct-1A, Oct-1L, and Oct-1X) which differed by their N-terminal regions. The corresponding transcripts start from alternative promoters and have different 5' exons (Figure 1A). First, we compared expression levels of Oct-1L, Oct-1X, and Oct-1A, and the total Oct-1 level in human tissues and cell cultures. The obtained data, presented in Figure 1B and C, show that the abundantly expressed Oct-1A is the main Oct-1 transcript, since in most cells its level roughly equals to that of the total Oct-1 mRNA. A high expression level of Oct-1L was found in brain and leukocytes, similar to that shown previously (31), and in the Burkitt's lymphoma cell lines Namalwa and Raji (Figure 1C), where it exceeds the level of Oct-1A. Oct-1X transcript was detected at a very low level (about 5%) relative to Oct-1A. Its highest level was found in leukocytes. The presence of transcripts containing the open reading frame for corresponding proteins in several human tissues and cell cultures was further demonstrated (Figure 1D).

Comparatively to Oct-1A, in the predicted Oct-1L isoform, the 18 N-terminal amino acids are replaced by an alternative 9 aa long peptide (Figure 1E). The shortest, Oct-1X, isoform lacks 21 N-terminal amino acids. An *in vitro* translation experiment demonstrated that electrophoretic mobility of all isoforms corresponded to those shown previously for the total Oct-1 (Figure 1F). Each Oct-1 isoform has its own specific sequences surrounding the first ATG codon and shares a high homology with the classic Kozak motif (Supplementary Figure S1).

To identify the endogenous Oct-1L and Oct-1A in human cell culture lines, we raised rabbit polyclonal antibodies against their unique N-terminal sequences, and looked for the presence of different Oct-1 isoforms in Namalwa, MOLT-4, and HeLa cells (Figure 1G). Oct-1A was detected in all the studied cell lines. In contrast, Oct-1L was actively synthesized in the Namalwa B-cell line where its content was even higher than that of Oct-1A, and at a lower level in MOLT-4 T-cell line, and was not detected in HeLa cells. These results correlated well with the level of Oct-1A and Oct-1L transcription in these cells. We could not distinguish the Oct-1X isoform by Western blot analysis as it has no unique sequence that could be used to raise antibodies against.

In summary, the above data demonstrate that distinct Oct-1 protein isoforms are expressed in human cells at different levels. The longest isoform, Oct-1A, is abundantly expressed in different tissues at the highest level while Oct-1X is expressed at a low level relative to Oct-1A.

The transcripts encoding the ubiquitous Oct-1A, and tissue-specific Oct-1L, were also detected in mice (32–34). The N-terminal regions of the predicted mouse protein isoforms are identical to the human ones, suggesting conservation of their function. Interestingly, mouse Oct-1L was also found to be highly expressed in B-cells (33). The N-terminal regions of A, L, and X isoforms could affect the functional activity of the protein due to different protein-

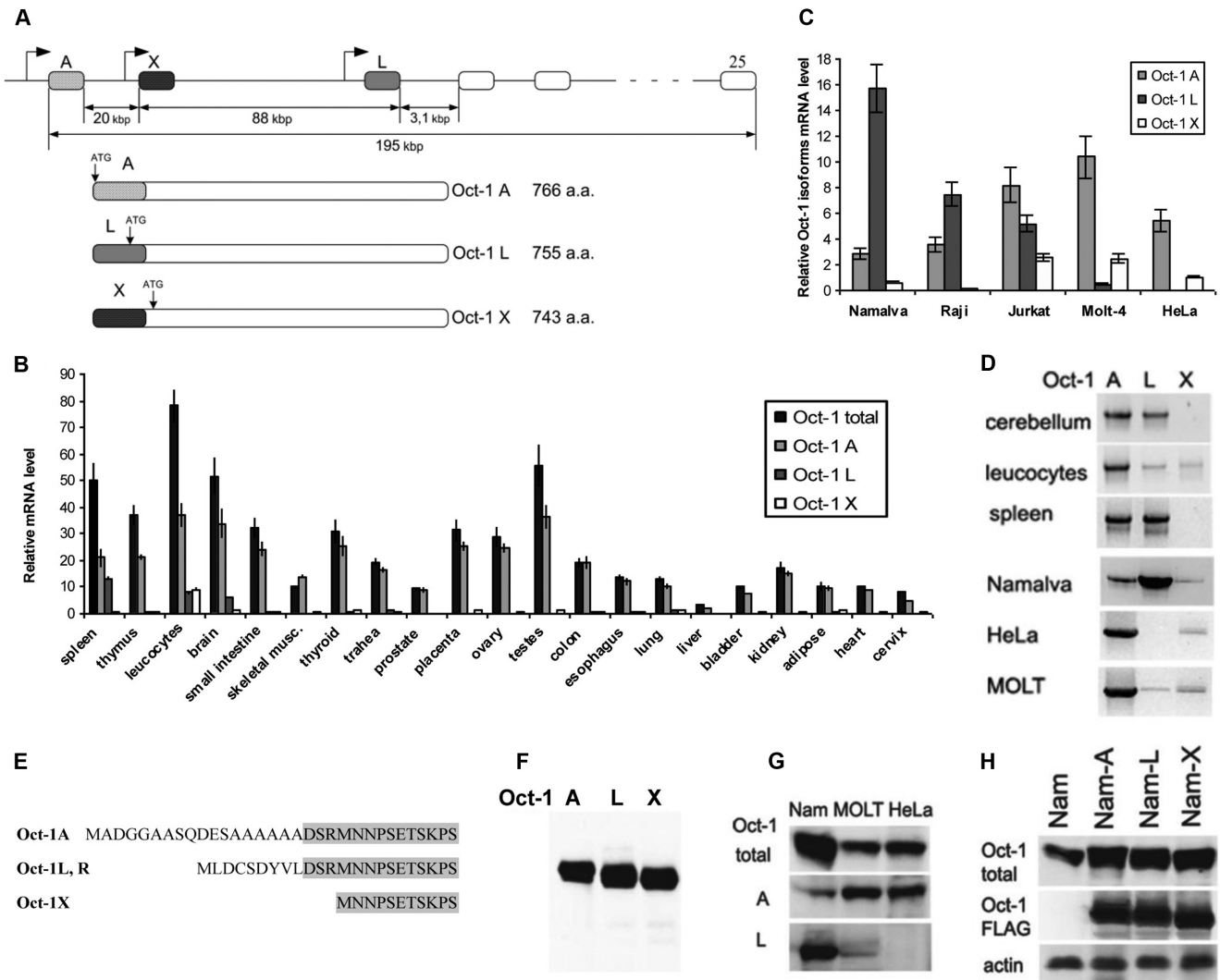


**Figure 1.** Expression of Oct-1 isoforms in human cells. (A) Schematic structure of Oct-1 alternative promoters and Oct-1A, Oct-1L, and Oct-1X transcripts with differ only by their 5'-terminal exons. Alternative exons are depicted as black or gray boxes. The transcription and translation starts are indicated. (B) Relative transcription level of the total Oct-1 mRNA and Oct-1 mRNA isoforms in human tissues measured by Real-Time PCR. The graphs show means  $\pm$  S.E.M. of three independent experiments. (C) Relative distribution of the Oct-1 mRNA isoforms in human cell lines measured by Real-Time PCR. The graphs show means  $\pm$  S.E.M. of three independent experiments. (D) The presence of transcripts encoding full-length Oct-1A, Oct-1L, and Oct-1X in human cells and tissues verified by PCR. (E) The amino acid sequence of N-terminal domains of Oct-1 isoforms. (F) Oct-1 isoforms synthesized *in vitro*. 1  $\mu$ g of DNA encoding full-length isoform in pcDNA3.1 vector was taken in reaction for *in vitro* transcription and translation. Western blot was developed by anti-FLAG antibodies. (G) The presence of Oct-1 isoforms in different cell lines. Western blot was developed with antibodies against total Oct-1, Oct-1A, and Oct-1L. (H) The endogenous Oct-1 and recombinant Oct-1 isoforms expressed in stably transformed Namalwa cell culture. Antibodies against Oct-1 (Oct-1 total) and against FLAG (Oct-1FLAG) were used for western blot. 10  $\mu$ g of protein extract was loaded to each well. Actin was used as a loading control.

protein interactions or presence of post-translational modification sites. A computational analysis with the Eukaryotic Linear Motif resource for Functional Sites in Proteins ([elm.eu.org](http://elm.eu.org)) revealed that the N-terminal domain of the L isoform has potential interaction sites with Rb and STAT5. The N-terminal region of Oct-A has potential modification sites for PIKK and Polo-like kinases, and an IAP-binding motif (IBM).

### Oct-1 isoforms control the overlapping gene expression patterns

To address the difference in functions of Oct-1 isoforms we determined gene expression profiles of the Namalwa Burkitt's lymphoma cell line and Namalwa cells stably transformed by lentivirus constructs expressing Oct-1A, Oct-1L, or Oct-1X linked with C-terminal 3xFLAG epitope. As verified by western blot analysis, each Oct-1 isoform was expressed in transgenic cells at an approximately equal level (Figure 1H). The amount of transgenic isoforms several times exceeded that of the endogenous protein and

was comparable with the level of Oct-1 observed in some tissues during development or in malignant cells (22,24,25,35).

Illumina HumanHT-12V4 microarrays were used to identify differentially expressed genes (DEGs) in cells transfected by the Oct-1 isoforms (GEO Database: GSE80287). Changes in the gene transcription were deemed as significant based on a fold change of  $\geq 2.0$  and a Benjamini-Hochberg adjusted  $P \leq 0.01$ . To verify the results of gene expression profile, they were confirmed by the RT-qPCR for several genes (Supplementary Figure S2A and B).

The highest number of DEGs was found for Oct-1X isoform (439), while the lowest (155) for Oct-1A (Figure 2A, Supplementary Table S1). The 5' regulatory regions of about half of the DEGs had the Oct-1 binding site (<http://www.genecards.org>). One hundred and one DEGs were common for all the three isoforms, suggesting that Oct-1L and Oct-1X may regulate expression of the Oct-1A targets.

Number of genes which changed their expression level in response to only one isoform more than two times (a fold change of  $\geq 2.0$  and a Benjamini-Hochberg adjusted  $P \leq 0.01$ ), comparatively to Namalwa, was lowest for Oct-1A, and much higher for Oct-1L and Oct-1X (Figure 2A). For some of the genes the transcription levels have changed significantly suggesting that these genes strongly responded to a particular isoform. We have also investigated target specificity of Oct-1 isoforms. To this end, we studied by the ChIP-qPCR analysis the presence of FLAG-tagged Oct-1 isoforms on the Oct-1 binding sites in the regulatory regions of DEGs. The specific binding of Oct-1 isoforms to a particular target site in the regulatory regions of the genes may be one of the mechanisms that determine the difference in the Oct-1 isoform gene targets (Supplementary Figure S2C).

Interestingly, DEGs common for several isoforms had a similar, unidirectional response (either *up* or *down*) to all of them, but the level of response was different (Figure 2B and C). The maximum increase in the expression level was up to 10 times (IGLL1 gene) and the maximum decrease was about 19 times (NBPF20 gene) (Figure 2B and C).

### Functional enrichment analysis of DEGs

To determine the biological processes, and the more relevant groups of DEGs regulated by Oct-1 isoforms, the functional enrichment analysis was performed by DAVID using GO (gene ontology) and KEGG pathways database. Three domains of gene ontology (biological process, cellular component, and molecular function) were analyzed for each isoform.

The more relevant biological processes are shown in Supplementary Table S2. A selection of highly up- and down-regulated processes is shown on Figure 3A–D. Most of the upregulated processes are similar for all three isoforms. The genes up-regulated for all three isoforms are related to such GO terms as ‘cell cycle’, ‘cell division’, ‘cell cycle regulation’, and ‘microtubule based process’. The more relevant up regulated KEGG pathway for all three isoforms is ‘cell cycle’ suggesting that the positive cell cycle regulation is their common function (Figure 3A and B). The Oct-1X differed from other isoforms, since it upregulated several additional processes. Among the most relevant up regulated GO terms are ‘DNA replication’, ‘DNA repair’, ‘RNA processing’, ‘DNA

recombination’, and ‘cellular response to stress’. The more relevant up regulated processes, which are annotated in the KEGG pathways database are ‘DNA replication’, ‘spliceosome’, and ‘base excision repair’ (Figure 3A and B).

All Oct-1 isoforms downregulated genes related to the immune system (‘immune response’ GO term and ‘natural killer mediated cytotoxicity’ of the KEGG database). The Oct-1L downregulated ‘antigen presentation via MHC class II’. Oct-1 isoforms also downregulated the ‘defense response’, ‘inflammatory response’, ‘programmed cell death’, and ‘negative regulation of cell death’ processes according to GO terms.

Among the downregulated processes are those that are connected with the following GO terms: ‘antigen processing and presentation’, ‘cytokine-cytokine receptor interaction’, and ‘cell adhesion molecules (CAMs)’. The DEGs belonging to these groups are shown in Supplementary Table S3.

The ‘antigen processing and presentation’ term includes a significant group of histocompatibility class I HLA genes. The cytokine and cytokine receptor group includes chemokines CCL4, CCL3, and chemokine receptors CXCR4 and CXCR7, interleukin receptors IL7R and IL21R, the IL10RB receptor subunit, and IFNAR2 interferon receptor. The downregulated TNF Receptor superfamily cytokines include TNFSF14, TNFRSF1B, and TNFRSF7 (CD27) receptors, TNFSF7 (CD70) ligand, and LTB. A member of the TGF-beta family of cytokines, INHBE, is among the most strongly downregulated genes. The genes encoding CAMs, transmembrane proteins responsible for cell adhesion and motility, include LPP and TSPAN8, which are some of the top downregulated genes (Figure 2C). Significantly decreased were levels of ICAM3, the ligand for leukocyte adhesion protein LFA-1, HMMR (hyaluronan-mediated motility receptor), and SIGLEC10 (sialic-acid binding Ig-like lectin 10). The decreased expression was observed for integrin beta-2 (CD18), the receptor for ICAM1-4, fibronectin, and VCAM1.

We have also identified about thirty transcription factors that change their expression level in response to Oct-1 (Supplementary Table S3). The presence of Oct-1 binding sites in the proximity of promoters of most of these factors (<http://www.genecards.org>) indicates that they could be directly regulated by Oct-1. Among them is FOXM1 gene, an important human proto-oncogene, expression of which increased more than 3 times in Oct-1X expressing cells. FOXM1 upregulation was detected in different human cancers (36).

### Oct-1 overexpression accelerates cell cycle progression

The functional enrichment analysis suggested that the positive cell cycle regulation is a common function for all three isoforms. Most of the top upregulated genes for all the studied Oct-1 isoforms are involved in the cell cycle regulation (Figure 2B), and the majority of them, like cell cycle regulated kinase AURKA, PBK, CCNB1 (cyclin B1), and CCNB2 (cyclin B2), are positive cell cycle regulators. An increased transcription was also observed for genes playing a critical role in various mitotic events, including the chromosome segregation, mitotic spindle organization, centrosome duplication, centrosome separation and maturation,

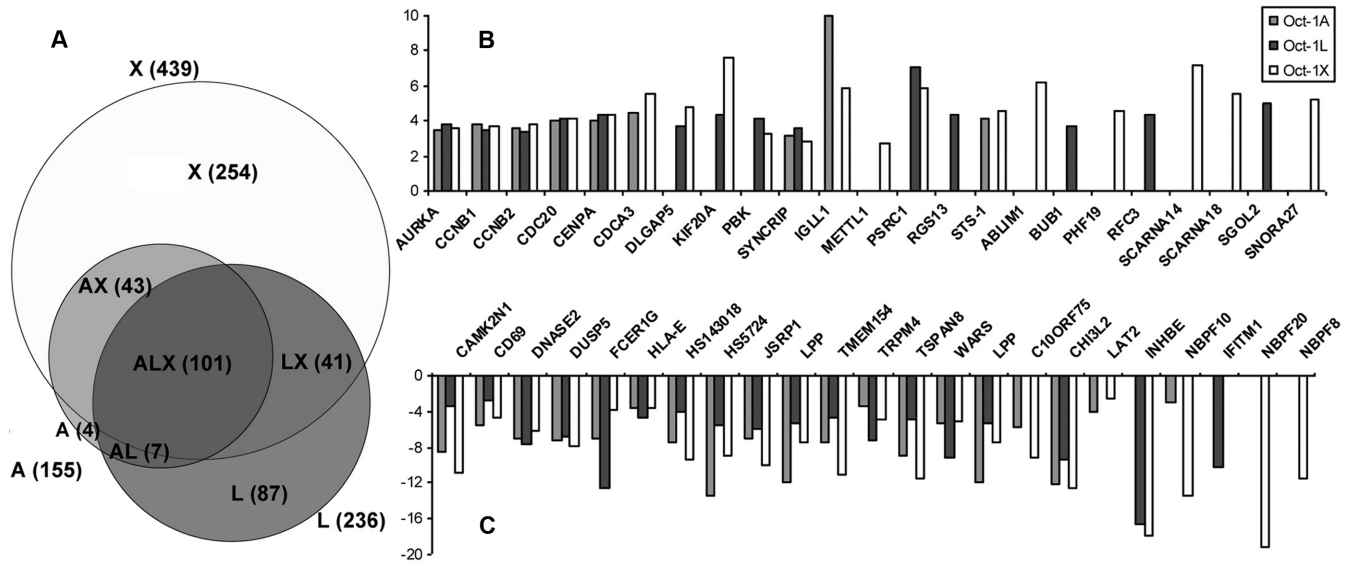


**Figure 2.** The results of gene expression analysis with Illumina HumanHT-12 microarray. (A) Venn diagram of differentially expressed genes identified from Namalwa cells transformed with different Oct-1 isoforms. 47 300 transcripts were tested. (B) The top 23 transcripts upregulated by Oct-1 isoforms. (C) The top 23 downregulated by Oct-1 isoforms.

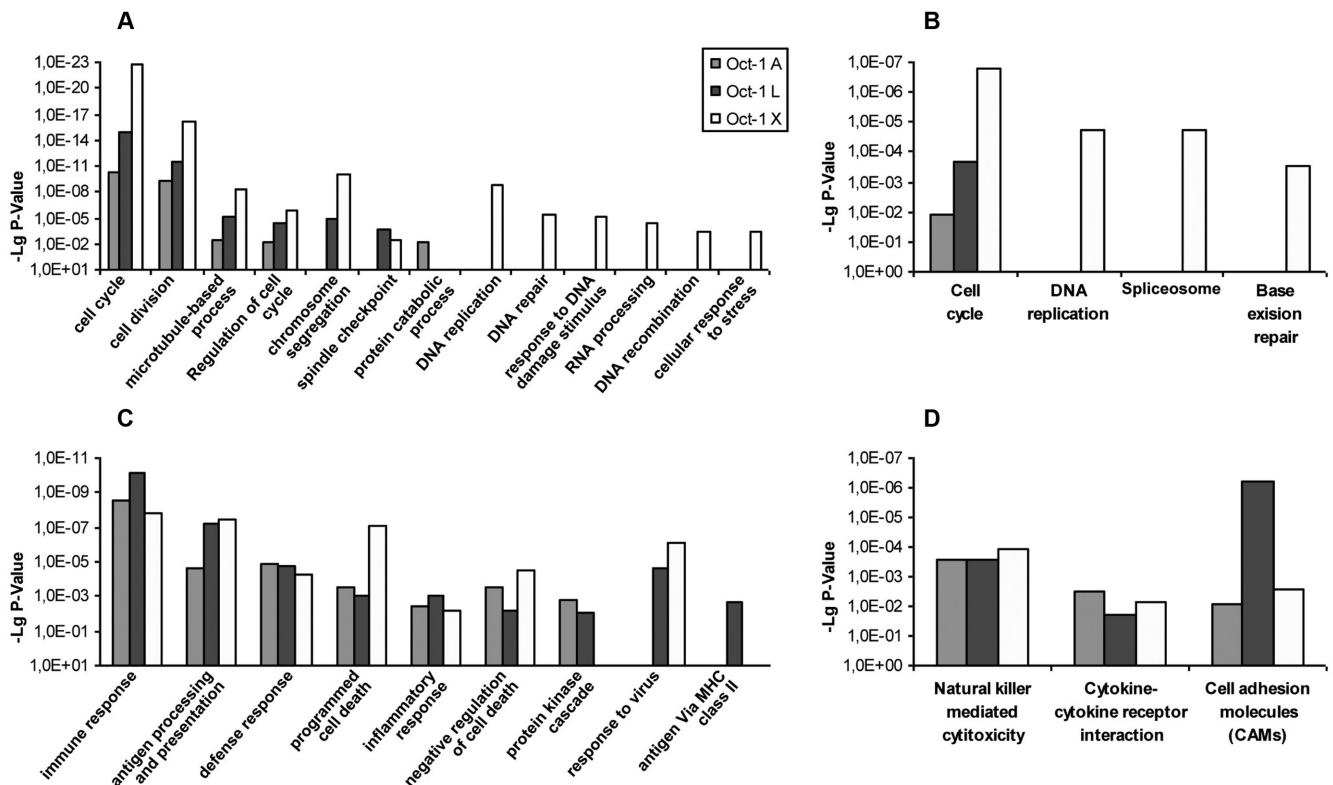


**Figure 3.** Functional enrichment analysis of differentially expressed genes for Oct-1 isoforms. (A and B) The more relevant Gene Ontology (GO) GOTERM\_BP\_FAT (biological process) (A) and KEGG Pathway (B) enrichment items of the upregulated DEGs. (C and D) The more relevant Gene ontology (GO) GOTERM\_BP\_FAT (biological process) (C) and KEGG Pathway (D) enrichment items of the downregulated DEGs.

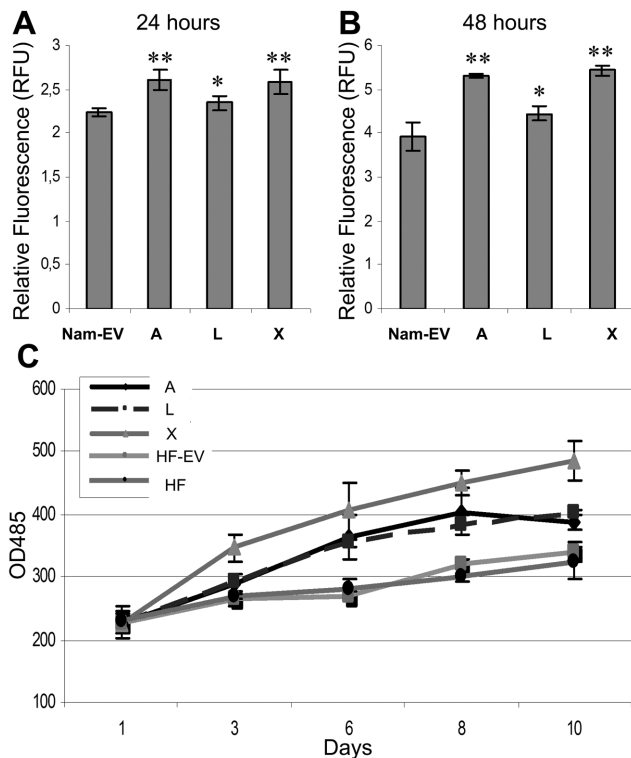


**Figure 4.** Oct-1 isoforms activate cell proliferation. (A, B) The rate of proliferation of Namalwa culture transfected with empty vector (Nam-EV) or FLAG tagged Oct-1 isoforms (Oct-1A, Oct-1L, Oct-1X) measured with CellTrace Violet kit at 24 and 48 h after seeding. Cells were stained according to the manufacturer's protocol and counted in a flow cytometer. Relative fluorescence (RFU) is proportional to the number of cell divisions and is calculated as the relation to the fluorescence on the day of seeding. The proportion of the necrotic cells (marked by the propidium iodide staining) in any sample did not exceed 1%. (C) CellTiter assay using primary human fibroblasts (HF), primary human fibroblasts transfected with empty vector (HF-EV), or Oct-1A, Oct-1L, Oct-1X isoforms. Cells were plated at 5000 per well in a 96-well plate in the final media volume of 100  $\mu$ l and monitored using CellTiter assay kit on 1, 3, 6, 8, and 10 day after seeding. The graphs show means  $\pm$  S.E.M. of three independent experiments. *t*-tests have been performed to compare the means (\* $P < 0.05$ , and \*\* $P < 0.01$ ).

spindle checkpoint, and cytokinesis (Table 1). On the other hand, transcription of several important negative cell cycle regulators, like cyclin-dependent kinase inhibitor 1A – CDKN1A and the antiproliferative protein TP53INP1, was significantly downregulated (Table 1).

To validate the above data, the experimental quantification of the cell cycle progression in cells with the Oct-1 overexpression was performed. The rate of the cell division was measured at 24 and 48 h, in the Namalwa cells transfected with an empty vector or a vector expressing Oct-1 isoforms using a CellTrace Violet Proliferation Kit (Invitrogen) (Figure 4). The obtained results demonstrated a statistically significant ( $P \leq 0.01$ ) increase in the number of the cell divisions due to a high expression level of Oct-1A, Oct-1X isoforms, and for Oct-1L isoform ( $P \leq 0.05$ ) already on the first day after seeding (Figure 4A). It further increased on the second day (Figure 4B).

Since Namalwa are human lymphoma cells that grow in suspension, we have verified this result on nonmalig-

nant cells. The early passage primary human fibroblasts were transfected with a FLAG-tagged Oct-1A, or Oct-L, or Oct-1X-encoding vector, or empty vector. All isoforms were efficiently expressed in transformant cells at approximately the same level (Supplementary Figure S3). On the second day, following the seeding, no significant difference in the rate of cell division between different cell lines was observed. Therefore, we measured the proliferation level for a longer time (10 days) with CellTiter assay (Promega) (Figure 4C). While both parental primary fibroblasts (HFs) and the HFs transfected with an empty vector demonstrated nearly identical growth rate, an overexpression of either of the isoforms led to an increase in proliferation. The difference was already noticeable after the third day following seeding.

Thus, in the Namalwa lymphoma cells and in the primary human fibroblasts, Oct-1 overexpression affects the cell cycle and accelerates cell cycle progression.

#### An elevated level of Oct-1 can either positively or negatively regulate apoptosis, depending upon the type of cell culture and the cell growth conditions

Functional enrichment analysis of DEGs demonstrated that Oct-1 isoforms negatively regulated both the programmed cell death and the negative regulation of cell death. The transcription of both the positive and the negative regulators of apoptosis was impaired (Supplementary Table S4). Those were such genes as caspase inhibitor CD27; TAX1BP1—the inhibitor of TNF-inducible apoptosis; BIRC3—inhibitor of apoptosis induced by serum deprivation; PIM2—serine/threonine protein kinase which prevents apoptosis and promotes cell survival; IFI6 which is induced by interferon and plays a critical role in apoptosis regulation; MCL1—anti-apoptotic protein of BCL2 family; apoptotic protector BNIP3, and others.

We investigated the resulting effect of Oct-1 on the apoptotic status of the cells. Namalwa cells transfected with empty vector or Namalwa cells with overexpressed Oct-1 isoforms were co-stained with Annexin V conjugated to Fluorescein and propidium iodide, with subsequent analysis by flow cytometry. We observed an increase of apoptotic cell numbers in population for all three isoforms (Figure 5A). This increase was not strong and the number of apoptotic cells in population did not increase substantially (from 4% to 8–9%), however the effect was statistically significant ( $P \leq 0.01$ ).

We also confirmed this result by measuring the level of caspase 3/7 activity in these cell lines. The analysis was performed using Caspase-Glo 3/7 Assay protocol. The analysis demonstrated a significant elevation of the basic level of caspase 3/7 activity in cells for each of the Oct-1 isoforms overexpressed (Figure 5B). Thus, two independent approaches demonstrated that the elevated level of Oct-1 in Namalwa cells increased their pro-apoptotic activity.

To investigate an effect of Oct-1 overexpression on apoptosis in the nonmalignant cells, the same experiments were performed on the human primary fibroblasts. Fibroblasts were seeded at different density (10 000 or 30 000 cells per well) and the caspase 3/7 activity was measured using a caspase-Glo 3/7 Assay at 24 h after the seeding. In cells

**Table 1.** Fold change of DEGs related to the cell cycle progression

Gene	Full Name	Oct 1A	Oct 1L	Oct 1X
<b>Up-regulated</b>				
ASPM	asp (abnormal spindle)	2.55	2.86	2.65
AURKA	aurora kinase A pseudogene 1	3.41	3.74	3.47
AURKB	aurora kinase B	–	–	4.1
BIRC5	baculoviral IAP repeat-containing 5	–	2.61	3.08
BUB1	budding uninhibited by benzimidazoles 1 homolog	–	3.6	–
BUB3	budding uninhibited by benzimidazoles 3 homolog	–	–	2.32
CDC20	cell division cycle 20	3.91	4.1	4.12
CDC25A	cell division cycle 25 homolog A	–	–	2.18
CDC25B	cell division cycle 25 homolog B	–	–	2.22
CDCA3	cell division cycle associated 3	4.41	–	5.27
CDCA5	cell division cycle associated 5	–	–	2.02
CDCA8	cell division cycle associated 8	3.03	–	3.41
CENPA	centromere protein A	3.93	4.34	4.26
CENPE	centromere protein E	–	3.38	3.08
CENPF	centromere protein F	3.25	–	3.94
CEP55	centrosomal protein	–	3.09	3.42
CCNB1	cyclin B1	3.75	3.46	3.61
CCNB2	cyclin B2	3.51	3.25	3.77
CCNF	cyclin F	–	2.79	3.29
CHEK1	CHK1 checkpoint homolog	–	–	3.08
DLGAP5	discs. large homolog-associated protein 5	–	3.61	4.69
ESPL1	extra spindle pole bodies homolog 1	–	–	3.29
FOXM1	forkhead box M1	–	–	3.37
HJURP	Holliday junction recognition protein	–	–	2.97
KIF11	kinesin family member 11	–	2.71	2.85
KIF20B	kinesin family member 20B	–	–	2.02
KIFC1	kinesin family member C1	–	–	2.89
LIG1	ligase I. DNA. ATP-dependent	–	–	2.7
MCM2	minichromosome maintenance complex component 2	–	–	3.19
MCM3	minichromosome maintenance complex component 3	–	–	1.94
MYC	v-myc myelocytomatosis viral oncogene homolog	–	2.58	–
NCAPG	non-SMC condensin I complex. subunit G	–	–	2.58
PBK	PDZ binding kinase	–	4.02	3.29
POLE	polymerase (DNA directed). epsilon	–	–	3.3
PA2G4	proliferation-associated 2G4. 38kDa; proliferation-associated 2G4 pseudogene 4	–	–	1.97
PSRC1	proline/serine-rich coiled-coil 1	–	6.98	5.62
RAD54L	RAD54-like	–	–	3.74
RANBP1	similar to RAN binding protein 1; RAN binding protein 1	–	–	1.93
SGOL2	shugoshin-like 2	–	4.77	–
SPC24	SPC24. NDC80 kinetochore complex component. homolog	–	–	2.58
TRIP13	thyroid hormone receptor interactor 13	–	–	2.68
TACC3	transforming. acidic coiled-coil containing protein 3	–	–	3.17
TPX2	TPX2. microtubule-associated. homolog	–	–	2.25
UBE2C	ubiquitin-conjugating enzyme E2C	3.87	2.59	3.55
UHRF1	ubiquitin-like with PHD and ring finger domains 1	–	–	2.37
ZWINT	ZW10 interactor	3.57	–	3.55
<b>Down-regulated</b>				
CDKN1A	cyclin-dependent kinase inhibitor 1A	–3.12	–2.56	–3.03
GAS7	growth arrest-specific 7	–	–6.25	–3.57
TP53INP1	tumor protein p53 inducible nuclear protein 1	–	–	–4.76

Genes upregulated or downregulated more than 2-fold are presented. Dashes (-) indicate that these genes were neither overexpressed at least two times nor downregulated by 50% after Oct-1 overexpression.

seeded at subconfluent conditions (10 000 cells per well), we did not observe a reliable effect of the Oct-1 overexpression on the caspase 3/7 activity in any of the cell lines transformed by the Oct-1 isoforms (Figure 5C). Contrary to this result, Oct-1 overexpression under overgrowth conditions (30 000 cells per well) caused a decrease of the level of the caspase 3/7 activity (Figure 5D). The effect of Oct-1A on the caspase 3/7 activity was more pronounced than for the other isoforms.

Thus, in line with the results of the functional enrichment analysis showing Oct-1 to be a negative regulator of both

the positive and negative regulators of the programmed cell death, our experimental data indicate that Oct-1 overexpression may positively or negatively regulate apoptosis depending on the cells type and growth conditions.

#### An elevated level of Oct-1 facilitates the pro-apoptotic effect of camptothecin on Namalwa cancer cells

In addition, we investigated an effect of a high level of Oct-1 expression on cell response to pro-apoptotic agents in Namalwa cancer cells. We used camptothecin (CPT), a topoisomerase I (TOP I) inhibitor, which binds to the TOP-I–



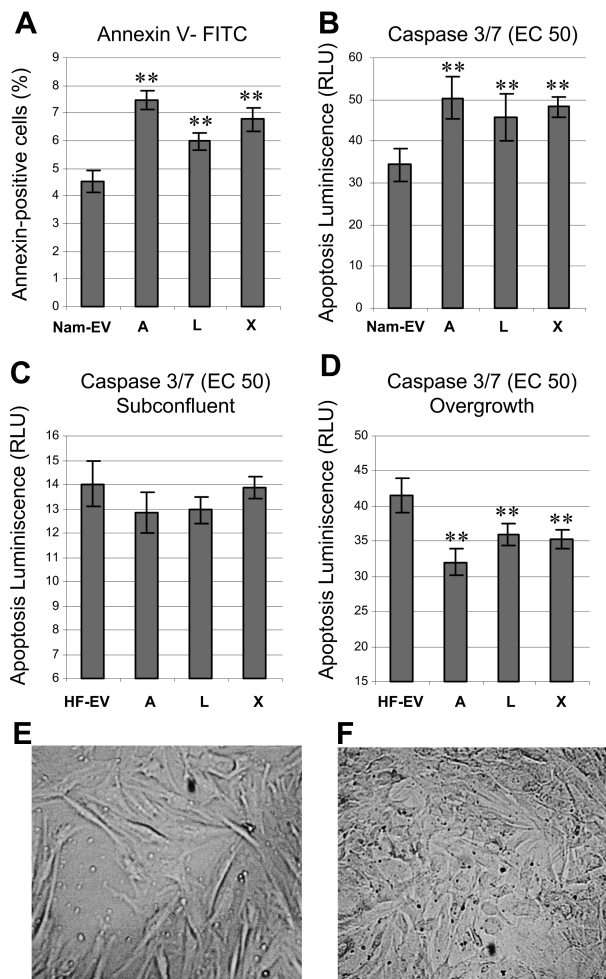


**Figure 5.** The influence of Oct-1 overexpression on apoptosis in Namalwa cells and human primary fibroblasts. (A) The effect of Oct-1 overexpression on the level of apoptosis in Namalwa cells. The empty vector transformed Namalwa cells (Nam-EV) were used as a control. The number of apoptotic cells is indicated on the Y-axis. Apoptosis was verified by double staining with the Annexin V-FITC and propidium iodide. The distribution of cells according to their fluorescence was registered for viable and apoptotic subpopulations, which were selected by size and granularity. All measurements were carried out on a Beckman Coulter Epix XL4 flow cytometer. The graphs show means  $\pm$  S.E.M. of three independent experiments. *t*-tests have been performed to compare the means. The asterisks indicate a *P* value of  $\leq 0.01$  relative to the empty vector transformed Namalwa cells value. (B) Caspase 3/7 level in the empty vector transformed Namalwa cells (Nam-EV) and in the cells stably transformed with Oct-1 isoforms, measured by a bioluminescent caspase assay. Cells were plated at 20 000 cells/well in 96-well plates in the final media volume of 100  $\mu$ L. The graphs show means  $\pm$  S.E.M. of three independent experiments. *t*-tests have been performed to compare the means. The asterisks indicate a *P* value of  $\leq 0.01$  relative to the control Namalwa cells value. (C) Caspase 3/7 level in the empty vector transformed primary human fibroblasts (HF-EV) and in the fibroblasts stably transformed with Oct-1 isoforms, measured by a bioluminescent caspase assay. Cells were plated at 10 000 cells/well in 96-well plates in the final media volume of 100  $\mu$ L. (D) Caspase 3/7 level in the empty vector transformed primary human fibroblasts (HF-EV) and in the fibroblasts stably transformed with Oct-1 isoforms, measured by a bioluminescent caspase assay. Cells were plated at 30 000 cells/well in 96-well plates in the final media volume of 100  $\mu$ L. The graphs show means  $\pm$  S.E.M. of three independent experiments. *t*-tests have been performed to compare the means. (\**P* < 0.05, and \*\**P* < 0.01). (E and F) Phase-contrast images of HF-EVs transformed with Oct-1A, plated at 10 000 (E) and 30 000 (F) per well. All measurements were carried and images were taken at 24 h after plating.

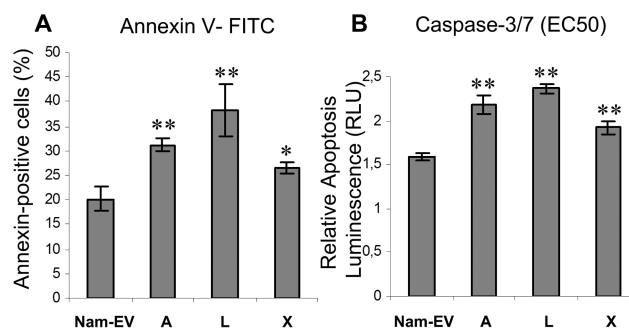


**Figure 6.** An effect of the Oct-1 overexpression on camptothecin induced apoptosis in Namalwa cells. (A) The camptothecin induced apoptosis in the empty vector transformed Namalwa cells (Nam-EV) and in cells stably transformed with Oct-1 isoforms. Apoptosis was verified as in Figure 5A. The number of apoptotic cells is indicated on the Y-axis. The graphs show means  $\pm$  S.E.M. of three independent experiments. *t*-tests have been performed to compare the means. (B) The Caspase 3/7 level in the empty vector transformed Namalwa cells (Nam-EV) and cells stably transformed with Oct-1 isoforms, treated with camptothecin, relative to the untreated cells, and measured by a bioluminescent caspase assay. Cells were plated at 20 000 cells/well on 96-well plates in the final media volume of 100  $\mu$ L. The graphs show means  $\pm$  S.E.M. of three independent experiments. *t*-tests have been performed to compare the means (\**P* < 0.05 and \*\**P* < 0.01).

DNA complex and prevents religation of DNA strands that results in the formation of DNA double-strand breaks leading to the cell cycle arrest and apoptosis. The camptothecin analogs are used in treatment of several different types of tumors.

The level of CPT induced apoptosis in the control and Oct-1 overexpressing Namalwa cell cultures was measured using Annexin V and propidium iodide staining with subsequent flow cytometry analysis. The results demonstrated an increase of apoptosis in cells transformed with each of the three isoforms (Figure 6A). The number of apoptotic cells in population increased substantially after Oct-1 overexpression. The measurement of caspase 3/7 activation confirmed this result (Figure 6B). In summary, an increase of Oct-1 level in Namalwa cells potentiates the pro-apoptotic effect of CPT.

#### Oct-1 overexpression leads to an increased glycolysis and decreased aerobic capacity of the Namalwa cells and primary human fibroblasts

In cells transformed by different Oct-1 isoforms we identified a number of downregulated DEGs, which regulate the mitochondrial oxidative phosphorylation and mitochondrial functioning (Supplemental Table S1). Among them were ATP5I, ATP5E, SLC25A5, SLC25A4, NDUFA3, TOMM7, TSPO, COX7A2L, MTHFD2, and others.

To understand whether high levels of Oct-1 isoforms have an effect on the cell metabolic state, we have measured the amount of ATP produced by the control and Oct-1 overexpressing Namalwa cells in either galactose- or glucose-supplemented media, as was described (36–38). In the galactose-supplemented media, the ATP level reflected the mitochondrial oxidative phosphorylation, since oxidation of galactose to pyruvate via glycolysis yields no ATP. As could be seen (Figure 7A), the amount of the ATP pro-

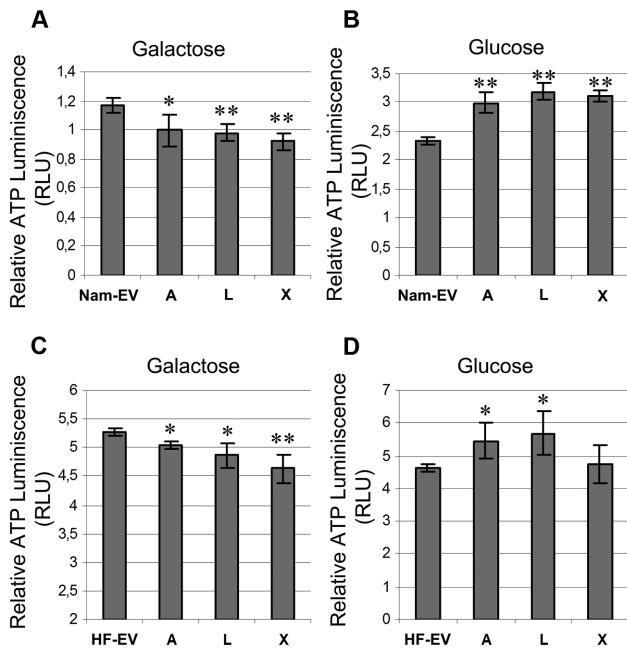


**Figure 7.** Measurement of the cellular ATP content in the Namalwa cells and primary human fibroblasts transformed with Oct-1 isoforms. (A and B) Namalwa cells transformed with an empty vector (Nam-EV) and cells stably transformed with Oct-1 isoforms grown on galactose (A) or glucose (B) supplemented media. (C and D) Primary human fibroblasts transformed with an empty vector (HF-EV) or stably transformed with Oct-1 isoforms overexpression grown on galactose (C) or glucose (D) supplemented media. Cells were plated at 20 000 cells/well in 96-well plates in the final media volume of 100  $\mu$ l. Cellular ATP concentrations were assessed with the CellTiter-Glo 2.0 Assay kit (Promega) according manufacturer's instructions and normalized to the number of viable cells (shown on the Y axis). The cell media was supplemented with 1 g/l of glucose or 10 mM galactose. The graphs show means  $\pm$  S.E.M. of three independent experiments. *t*-tests have been performed to compare the means (\* $P < 0.05$  and \*\* $P < 0.01$ ).

duced by the Oct-1 transformed cells was decreased comparatively to the control, suggesting an impairment of mitochondrial functioning. On the other hand, when grown in the glucose-supplemented media, the Oct-1 transformed cells produced more ATP than Namalwa cells, suggesting an increase of glycolysis level (Figure 7B).

Interestingly, the same data were obtained on the human primary fibroblasts (Figure 7C and D). The only exception was the Oct-1X isoform which did not cause an alteration of the ATP level in the glucose containing media.

Thus, our data demonstrated that Oct-1 overexpression induced metabolic alterations that increased glycolysis and suppressed mitochondrial metabolism. In several publications the involvement of Oct-1 in the cellular metabolism was demonstrated. Shakya *et al.* (26) demonstrated that low level of Oct1 induces a coordinated metabolic shift in the embryonic mouse fibroblasts: mitochondrial activity and amino acid oxidation are increased, while glucose metabolism is reduced (26). So, these studies are complementary to each other. Ansari *et al.* (39) showed that Oct-1 plays a critical role in the miR-451 expression (39). The AMPK activation by glucose deprivation leads to an inactivation of Oct-1 *via* a direct phosphorylation at serine 335,

which leads to the inhibition of the miR-451 transcription. Inhibition of miR-451 in turn results in a sustained AMPK activation, and a robust response to glucose deprivation. Together with our study, which reveals a group of metabolic genes regulated by Oct-1, this study uncovers the pathways underlining Oct-1 involvement in the regulation of cellular metabolism.

## DISCUSSION

Here, we demonstrate that different Oct-1 protein isoforms are present in human cells. The abundantly expressed Oct-1A, which has the longest N-terminal domain is the major Oct-1 isoform comprising almost all Oct-1, in most of the tissues. Oct-1L is highly expressed in the Namalwa Burkitt's lymphoma B-cells, where its level exceeds that of Oct-1A, but in most of the other tissues its expression is low. Interestingly, in mice Oct-1L is also tissue-specific and its highest level was observed in the normal B-cells (33). The Oct-1X is expressed at a low level comparatively to Oct-1A. This is an important fact, since at present time this isoform is considered as a 'canonical' Oct-1 sequence and is used in the majority of studies devoted to investigation of Oct-1 functions (14,23,25,40–46).

Microarray analysis showed that Oct-1A isoform controls the expression of a core set of Oct-1 sensitive genes most of which are common to all three studied isoforms. Oct-1L and Oct-1X do not have an effect on the common target genes opposite to that of Oct-1A, but rather modulate the rate of their activation or repression. It correlates well with the previously obtained data demonstrating that Oct-1 isoforms elicit a varying level of activation of the same target genes *in vitro* (29,30).

The Oct-1L and Oct-1X isoforms control a wider set of genes than Oct-1A. Our data demonstrated that the sets of expressed genes as well as processes controlled by Oct-1X significantly differ from the other isoforms. In particular, Oct-1X mostly activated genes for DNA replication and reparation, DNA recombination, response to DNA damage, and the cellular response to stress. The role of Oct-1X in activation of the stress response and DNA damage response genes correlated well with the data demonstrating that the recombinant 743 aa form of Oct-1 (which corresponds to Oct-1X) promotes resistance to cell stress (20). The role of Oct-1 in the regulation of the genotoxic and oxidative stress response is also described (23). Our data suggest that it is Oct-1X, and not the other isoforms, which is involved in the stress response regulation. It is possible, that Oct-1X is activated in cells only under specific environmental conditions.

The positive effect of a high level of Oct-1 on tumor progression was demonstrated in several studies (22,24,25,47,48) and is widely discussed (49). Our data, at least partially, uncover a mechanism of this effect. We have demonstrated that while having significant differences in the gene regulation patterns, all three isoforms activate genes responsible for the positive regulation of the cell cycle progression and active proliferation. Moreover, the ability of high expression level of Oct-1 to activate proliferation was demonstrated both in the Namalwa cells and in the primary human fibroblasts, suggesting that Oct-1 is a strong activa-

tor of cellular growth. Thus, tumor growth should be accelerated upon an activation of the Oct-1 gene.

The inhibition by Oct-1 of the expression of adhesion genes should facilitate detachment of tumor cells from the primary tumor. As a result, their increased motility may be an important factor in tumor invasiveness and metastatic potential. Tumor cells in the metastases frequently escape an attack by cytolytic T lymphocytes due to a loss of the HLA class I antigens (50). An enhanced Oct-1 level just may lead to the latter. The HLA class I antigen down-regulation is a frequent event in cervical carcinomas (50–52). The impairment of cytokine–cytokine receptor interaction provides an escape for a cell from the control of the surrounding cells and the whole organism.

Our data also demonstrate that human Oct-1 overexpression leads to a shift of cellular metabolism from the oxidative to anaerobic glycolytic type. It was demonstrated both in the Namalwa cells and in the primary human fibroblasts. These data complement the results demonstrating that mouse Oct-1 regulates a number of metabolic genes involved in a switch from oxidative to anaerobic glycolytic metabolism, and Oct-1 knockdown shifts the cell metabolism to the oxidative type (26).

Finally, we have observed among the DEGs a significant number of the transcription factor genes. In particular, we have observed a decrease in expression of such tumor suppressor genes as AXUD1, EGR1, IRF1, TP53INP1, and an increase in expression of a well-known proto-oncogene FOXM1.

Overexpression of all the studied Oct-1 isoforms impairs transcription of a number of positive and negative regulators of apoptosis that cumulatively leads to a moderate increase of apoptosis level in the Namalwa Burkitt's lymphoma cells. Nevertheless, Namalwa cells with a high Oct-1 level actively proliferate, since their proliferative rate is even higher than the rate of the programmed cell death. One example of a powerful oncogene which accelerates cell divisions and increases the level of apoptosis is c-Myc (53). On the other hand, in the primary human fibroblasts grown at high density, the level of apoptosis is decreased under Oct-1 overexpression, while at a low density of the seeded cells, it is not affected. Taken together, these results suggest that Oct-1 is not a strong activator of apoptosis but mainly could be a switch factor which shifts apoptosis level depending on the cell type and the growth conditions.

We have also demonstrated that a high level of Oct-1 potentiates the pro-apoptotic effect of camptothecin on the Namalwa cells. If this effect could be observed in different tumor cells, a high level of Oct-1 in tumors may have a prognostic significance for effectiveness of treatment with camptothecin analogs.

The processes controlled by Oct-1 including the rate of cellular divisions, apoptosis, and the functional connections between different cells uncovered in this study are important at the embryonic stage of development. Indeed, the Oct-1 null mice die during early embryogenesis (54) and Oct-1 was shown to play an important role in various developmental processes (54–56). In *Xenopus* Oct-1 is involved in the specification and differentiation of neural cells (35,57). A high level of Oct-1 in stem cells and at the early embryonic stages is found in mice (35). In *Xenopus* during embry-

onic development, Oct-1 is expressed in cells that undergo massive proliferation while the differentiation and loss of pluripotency is accompanied by a decline in Oct-1 expression (35,57). Evidently, the increase of Oct-1 level in adult cells diminishes their differentiation level and potentiates pluripotency. These functions of Oct-1 at embryonic stage could be connected to its tumorigenic role.

The capacity of Oct-1 to regulate a wide range of functionally distinct genes and processes is based on its ability to bind to distinct DNA sites (5–10), to interact with various transcription factors (14,19,58–61) and to undergo multiple post translational modifications (41,62,63). Our study demonstrates that the existence of Oct-1 isoforms which vary in length and sequence at the N-terminus of the protein, also contributes in surprising diversity of Oct-1 functions in transcription regulation.

## SUPPLEMENTARY DATA

Supplementary Data are available at NAR Online.

## ACKNOWLEDGEMENTS

Authors are grateful to the Center of Shared Use of Equipment ‘Genome’ at the Engelhardt Institute of Molecular Biology, Russian Academy of Sciences, for access to various equipment and help in its use.

## ACCESSION NUMBERS

Oct-1X mRNA and KT438684.1.

## FUNDING

Russian Science Foundation [14-15-01032 to S.G.]; the microarray analysis was supported by the program ‘Molecular and Cell Biology’ of the Russian Academy of Sciences. Funding for open access charge: Russian Science Foundation.

*Conflict of interest statement.* None declared.

## REFERENCES

- Zhang,X., Ma,Y., Liu,X., Zhou,Q. and Wang,X.J. (2013) Evolutionary and functional analysis of the key pluripotency factor Oct4 and its family proteins. *J. Genet. Genomics*, **40**, 399–412.
- Sturm,R.A., Das,G. and Herr,W. (1988) The ubiquitous octamer-binding protein Oct-1 contains a POU domain with a homeo box subdomain. *Genes Dev.*, **2**, 1582–1599.
- Sytina,E.V. and Pankratova,E.V. (2003) Transcription factor Oct-1: plasticity and multiplicity of function. *Mol. Biol. (Mosk.)* **37**, 637–648.
- Zhao,F.Q. (2013) Octamer-binding transcription factors: genomics and functions. *Front. Biosci. (Landmark edition)*, **18**, 1051–1071.
- Stepchenko,A.G. (1992) [Interaction of Oct-binding transcription factors with a large series of “noncanonical” oct-sequences. Primary sequence of murine Oct-2B cDNA]. *Dokl. Akad. Nauk*, **325**, 175–178.
- Verrijzer,C.P., Alkema,M.J., van Weperen,W.W., Van Leeuwen,H.C., Strating,M.J. and van der Vliet,P.C. (1992) The DNA binding specificity of the bipartite POU domain and its subdomains. *EMBO J.*, **11**, 4993–5003.
- Stepchenko,A.G. (1994) Noncanonical Oct-sequences are targets for mouse Oct-2B transcription factor. *FEBS Lett.*, **337**, 175–178.
- Stepchenko,A.G., Luchina,N.N. and Pankratova,E.V. (1997) Cysteine 50 of the POU H domain determines the range of targets recognized by POU proteins. *Nucleic Acids Res.*, **25**, 2847–2853.

9. Stepchenko, A.G., Luchina, N.N. and Polanovsky, O.L. (1997) Conservative Val47 residue of POU homeodomain: role in DNA recognition. *FEBS Lett.*, **412**, 5–8.
10. Tomilin, A., Remenyi, A., Lins, K., Bak, H., Leidel, S., Vriend, G., Wilmanns, M. and Scholer, H.R. (2000) Synergism with the coactivator OBF-1 (OCA-B, BOB-1) is mediated by a specific POU dimer configuration. *Cell*, **103**, 853–864.
11. Fletcher, C., Heintz, N. and Roeder, R.G. (1987) Purification and characterization of OTF-1, a transcription factor regulating cell cycle expression of a human histone H2b gene. *Cell*, **51**, 773–781.
12. Yang, J., Muller-Immergluck, M.M., Seipel, K., Janson, L., Westin, G., Schaffner, W. and Pettersson, U. (1991) Both Oct-1 and Oct-2A contain domains which can activate the ubiquitously expressed U2 snRNA genes. *EMBO J.*, **10**, 2291–2296.
13. Janson, L., Weller, P. and Pettersson, U. (1989) Nuclear factor I can functionally replace transcription factor Sp1 in a U2 small nuclear RNA gene enhancer. *J. Mol. Biol.*, **205**, 387–396.
14. Strom, A.C., Forsberg, M., Lillhager, P. and Westin, G. (1996) The transcription factors Sp1 and Oct-1 interact physically to regulate human U2 snRNA gene expression. *Nucleic Acids Res.*, **24**, 1981–1986.
15. Wu, G.D., Lai, E.J., Huang, N. and Wen, X. (1997) Oct-1 and CCAAT/enhancer-binding protein (C/EBP) bind to overlapping elements within the interleukin-8 promoter. The role of Oct-1 as a transcriptional repressor. *J. Biol. Chem.*, **272**, 2396–2403.
16. Delhase, M., Castrillo, J.L., de la Hoya, M., Rajas, F. and Hooghe-Peters, E.L. (1996) AP-1 and Oct-1 transcription factors down-regulate the expression of the human PIT1/GHF1 gene. *J. Biol. Chem.*, **271**, 32349–32358.
17. Chandran, U.R., Attardi, B., Friedman, R., Zheng, Z., Roberts, J.L. and DeFranco, D.B. (1996) Glucocorticoid repression of the mouse gonadotropin-releasing hormone gene is mediated by promoter elements that are recognized by heteromeric complexes containing glucocorticoid receptor. *J. Biol. Chem.*, **271**, 20412–20420.
18. Chandran, U.R., Warren, B.S., Baumann, C.T., Hager, G.L. and DeFranco, D.B. (1999) The glucocorticoid receptor is tethered to DNA-bound Oct-1 at the mouse gonadotropin-releasing hormone distal negative glucocorticoid response element. *J. Biol. Chem.*, **274**, 2372–2378.
19. Voss, J.W., Wilson, L. and Rosenfeld, M.G. (1991) POU-domain proteins Pit-1 and Oct-1 interact to form a heteromeric complex and can cooperate to induce expression of the prolactin promoter. *Genes Dev.*, **5**, 1309–1320.
20. Tantin, D., Schild-Poulter, C., Wang, V., Hache, R.J. and Sharp, P.A. (2005) The octamer binding transcription factor Oct-1 is a stress sensor. *Cancer Res.*, **65**, 10750–10758.
21. Kang, J., Gemberling, M., Nakamura, M., Whitby, F.G., Handa, H., Fairbrother, W.G. and Tantin, D. (2009) A general mechanism for transcription regulation by Oct1 and Oct4 in response to genotoxic and oxidative stress. *Genes Dev.*, **23**, 208–222.
22. Maddox, J., Shakya, A., South, S., Shelton, D., Andersen, J.N., Chidester, S., Kang, J., Gligorich, K.M., Jones, D.A., Spangrude, G.J. *et al.* (2012) Transcription factor Oct1 is a somatic and cancer stem cell determinant. *PLoS Genet.*, **8**, e1003048.
23. Kang, J., Shakya, A. and Tantin, D. (2009) Stem cells, stress, metabolism and cancer: a drama in two Octs. *Trends Biochem. Sci.*, **34**, 491–499.
24. Xiao, S., Liao, S., Zhou, Y., Jiang, B., Li, Y. and Xue, M. (2014) High expression of octamer transcription factor 1 in cervical cancer. *Oncol. Lett.*, **7**, 1889–1894.
25. Qian, J., Kong, X., Deng, N., Tan, P., Chen, H., Wang, J., Li, Z., Hu, Y., Zou, W., Xu, J. *et al.* (2015) OCT1 is a determinant of synbindin-related ERK signalling with independent prognostic significance in gastric cancer. *Gut*, **64**, 37–48.
26. Shakya, A., Cooksey, R., Cox, J.E., Wang, V., McClain, D.A. and Tantin, D. (2009) Oct1 loss of function induces a coordinate metabolic shift that opposes tumorigenicity. *Nat. Cell Biol.*, **11**, 320–327.
27. Pankratova, E.V., Sytina, E.V., Luchina, N.N. and Krivega, I.V. (2003) The regulation of the Oct-1 gene transcription is mediated by two promoters. *Immunol. Lett.*, **88**, 15–20.
28. Pankratova, E., Sytina, E. and Polanovsky, O. (2006) Autoregulation of Oct-1 gene expression is mediated by two octa-sites in alternative promoter. *Biochimie*, **88**, 1323–1329.
29. Krylova, I.D., Portseva, T.N., Georgieva, S.G., Stepchenko, A.G. and Pankratova, E.V. (2013) New isoform of Oct-1 transcription factor is transcribed from alternative promoter. *Mol. Biol. (Mosk.)*, **47**, 552–558.
30. Das, G. and Herr, W. (1993) Enhanced activation of the human histone H2B promoter by an Oct-1 variant generated by alternative splicing. *J. Biol. Chem.*, **268**, 25026–25032.
31. Luchina, N.N., Krivega, I.V. and Pankratova, E.V. (2003) Human Oct-1L isoform has tissue-specific expression pattern similar to Oct-2. *Immunol. Lett.*, **85**, 237–241.
32. Suzuki, N., Peter, W., Ciesiolka, T., Gruss, P. and Scholer, H.R. (1993) Mouse Oct-1 contains a composite homeodomain of human Oct-1 and Oct-2. *Nucleic Acids Res.*, **21**, 245–252.
33. Pankratova, E.V., Deyev, I.E., Zhenilo, S.V. and Polanovsky, O.L. (2001) Tissue-specific isoforms of the ubiquitously transcription factor Oct-1. *Mol. Genet. Genomics: MGG*, **266**, 239–245.
34. Stepchenko, A.G. (1992) The nucleotide sequence of mouse OCT-1 cDNA. *Nucleic Acids Res.*, **20**, 1419.
35. Veenstra, G.J., Beumer, T.L., Peterson-Maduro, J., Stegeman, B.I., Karg, H.A., van der Vliet, P.C. and Destree, O.H. (1995) Dynamic and differential Oct-1 expression during early Xenopus embryogenesis: persistence of Oct-1 protein following down-regulation of the RNA. *Mech. Dev.*, **50**, 103–117.
36. Laoukili, J., Stahl, M. and Medema, R. H. (2007) FoxM1: At the crossroads of ageing and cancer. *Biochim. Biophys. Acta*, **1775**, 92–102.
37. Marroquin, L.D., Hynes, J., Dykens, J.A., Jamieson, J.D. and Will, Y. (2007) Circumventing the Crabtree effect: replacing media glucose with galactose increases susceptibility of HepG2 cells to mitochondrial toxicants. *Toxicol. Sci.*, **97**, 539–547.
38. Rossignol, R., Gilkerson, R., Aggeler, R., Yamagata, K., Remington, S.J. and Capaldi, R.A. (2004) Energy substrate modulates mitochondrial structure and oxidative capacity in cancer cells. *Cancer Res.*, **64**, 985–993.
39. Ansari, K.I., Ogawa, D., Rooj, A.K., Lawler, S.E., Krichevsky, A.M., Johnson, M.D., Chiocca, E.A., Bronisz, A. and Godlewski, J. (2015) Glucose-based regulation of miR-451/AMPK signaling depends on the OCT1 transcription factor. *Cell Rep.*, **11**, 902–909.
40. Tanaka, M. and Herr, W. (1990) Differential transcriptional activation by Oct-1 and Oct-2: interdependent activation domains induce Oct-2 phosphorylation. *Cell*, **60**, 375–386.
41. Lee, L., Stollar, E., Chang, J., Grossmann, J.G., O'Brien, R., Ladbury, J., Carpenter, B., Roberts, S. and Luisi, B. (2001) Expression of the Oct-1 transcription factor and characterization of its interactions with the Bob1 coactivator. *Biochemistry*, **40**, 6580–6588.
42. Schild-Poulter, C., Shih, A., Tantin, D., Yarymowich, N.C., Soubeyrand, S., Sharp, P.A. and Hache, R.J. (2007) DNA-PK phosphorylation sites on Oct-1 promote cell survival following DNA damage. *Oncogene*, **26**, 3980–3988.
43. Schild-Poulter, C., Shih, A., Yarymowich, N.C. and Hache, R.J. (2003) Down-regulation of histone H2B by DNA-dependent protein kinase in response to DNA damage through modulation of octamer transcription factor 1. *Cancer Res.*, **63**, 7197–7205.
44. dela Paz, N.G., Simeonidis, S., Leo, C., Rose, D.W. and Collins, T. (2007) Regulation of NF-kappaB-dependent gene expression by the POU domain transcription factor Oct-1. *J. Biol. Chem.*, **282**, 8424–8434.
45. Wang, P., Wang, Q., Sun, J., Wu, J., Li, H., Zhang, N., Huang, Y., Su, B., Li, R.K., Liu, L. *et al.* (2009) POU homeodomain protein Oct-1 functions as a sensor for cyclic AMP. *J. Biol. Chem.*, **284**, 26456–26465.
46. Chiefari, E., Arcidiacono, B., Possidente, K., Iiritano, S., Ventura, V., Pandolfo, R., Brunetti, F.S., Greco, M., Foti, D. and Brunetti, A. (2013) Transcriptional regulation of the HMGAI gene by octamer-binding proteins Oct-1 and Oct-2. *PLoS One*, **8**, e83969.
47. Wang, Y.P., Song, G.H., Chen, J., Xiao, C., Li, C., Zhong, L., Sun, X., Wang, Z.W., Deng, G.L., Yu, F.D. *et al.* (2015) Elevated OCT1 participates in colon tumorigenesis and independently predicts poor prognoses of colorectal cancer patients. *Tumour Biol.*, doi:10.1007/s13277-015-4080-0.
48. Liu, Y., Wang, Y., Sun, X., Mei, C., Wang, L., Li, Z. and Zha, X. (2015) miR-449a promotes liver cancer cell apoptosis by down-regulation of Calpain6 and POU2F1. *Oncotarget*, **7**, 13491–13501.

49. Vázquez-Arreguín, K. and Tantin, D. (2016) The Oct1 transcription factor and epithelial malignancies: Old protein learns new tricks. *Biochim. Biophys. Acta*, doi:10.1016/j.bbagr.2016.02.007.
50. Garrido, F., Cabrera, T., Concha, A., Glew, S., Ruiz-Cabello, F. and Stern, P.L. (1993) Natural history of HLA expression during tumour development. *Immunol. Today*, **14**, 491–499.
51. Keating, P.J., Cromme, F.V., Duggan-Keen, M., Snijders, P.J., Walboomers, J.M., Hunter, R.D., Dyer, P.A. and Stern, P.L. (1995) Frequency of down-regulation of individual HLA-A and -B alleles in cervical carcinomas in relation to TAP-1 expression. *Br. J. Cancer*, **72**, 405–411.
52. Bartholomew, J.S., Glenville, S., Sarkar, S., Burt, D.J., Stanley, M.A., Ruiz-Cabello, F., Chengang, J., Garrido, F. and Stern, P.L. (1997) Integration of high-risk human papillomavirus DNA is linked to the down-regulation of class I human leukocyte antigens by steroid hormones in cervical tumor cells. *Cancer Res.*, **57**, 937–942.
53. Wang, C., Tai, Y., Lisanti, M.P. and Liao, D.J. (2011) c-Myc induction of programmed cell death may contribute to carcinogenesis: a perspective inspired by several concepts of chemical carcinogenesis. *Cancer Biol. Ther.*, **11**, 615–626.
54. Sebastiano, V., Dalvai, M., Gentile, L., Schubart, K., Sutter, J., Wu, G.M., Tapia, N., Esch, D., Ju, J.Y., Hubner, K. *et al.* (2010) Oct1 regulates trophoblast development during early mouse embryogenesis. *Development (Cambridge, England)*, **137**, 3551–3560.
55. Donner, A.L., Episkopou, V. and Maas, R.L. (2007) Sox2 and Pou2f1 interact to control lens and olfactory placode development. *Dev. Biol.*, **303**, 784–799.
56. Kiyota, T., Kato, A., Altmann, C.R. and Kato, Y. (2008) The POU homeobox protein Oct-1 regulates radial glia formation downstream of Notch signaling. *Dev. Biol.*, **315**, 579–592.
57. Veenstra, G.J., Peterson-Maduro, J., Mathu, M.T., van der Vliet, P.C. and Destree, O.H. (1998) Non-cell autonomous induction of apoptosis and loss of posterior structures by activation domain-specific interactions of Oct-1 in the *Xenopus* embryo. *Cell Death Differ.*, **5**, 774–784.
58. Luo, Y. and Roeder, R.G. (1995) Cloning, functional characterization, and mechanism of action of the B-cell-specific transcriptional coactivator OCA-B. *Mol. Cell. Biol.*, **15**, 4115–4124.
59. Sauter, P. and Matthias, P. (1997) The B cell-specific coactivator OBF-1 (OCA-B, Bob-1) is inducible in T cells and its expression is dispensable for IL-2 gene induction. *Immunobiology*, **198**, 207–216.
60. Sauter, P. and Matthias, P. (1998) Coactivator OBF-1 makes selective contacts with both the POU-specific domain and the POU homeodomain and acts as a molecular clamp on DNA. *Mol. Cell. Biol.*, **18**, 7397–7409.
61. Strubin, M., Newell, J.W. and Matthias, P. (1995) OBF-1, a novel B cell-specific coactivator that stimulates immunoglobulin promoter activity through association with octamer-binding proteins. *Cell*, **80**, 497–506.
62. Roberts, S.B., Segil, N. and Heintz, N. (1991) Differential phosphorylation of the transcription factor Oct1 during the cell cycle. *Science (New York, N.Y.)*, **253**, 1022–1026.
63. Kang, J., Goodman, B., Zheng, Y. and Tantin, D. (2011) Dynamic regulation of Oct1 during mitosis by phosphorylation and ubiquitination. *PLoS One*, **6**, e23872.